

Article

Reduction in the Volumetric Wear of a Ball Polishing Tool Using Ultrasonic-Vibration-Assisted Polishing Process

Fang-Jung Shiou *, Zhao-Li Ding and Sun-Peng Lin

Department of Mechanical Engineering, National Taiwan University of Science and Technology, Taipei 104, Taiwan

* Correspondence: shiou@mail.ntust.edu.tw; Tel.: +886-2-2737-6543; Fax: +886-2-2737-6460

Abstract: Ultraprecision freeform polishing using a bonnet or a felt ball mounted on a polishing head plays an important role in the mold and lens production industries. The volumetric wear of a bonnet or a felt polishing ball is still a problem to be solved. The objective of this study was to develop an ultrasonic-vibration-assisted ball polishing process on a CNC machining center to improve the surface roughness of a STAVAX mold steel and to reduce the volumetric wear of the polishing ball. The optimal combination of the ultrasonic-vibration-assisted ball polishing parameters for a plane surface was determined by conducting the Taguchi L18 matrix experiments, ANOVA analysis, and verification experiments. The surface roughness of the polished specimens was improved from the burnished surface roughness of Ra 0.122 μm to Ra 0.022 μm . In applying the optimal plane surface ball burnishing and vibration-assisted spherical polishing parameters sequentially to a fine-milled and burnished aspherical lens surface carrier on a five-axis machining center, the surface roughness of Ra 0.014 μm was obtainable. The improvement in the volumetric wear of the polishing ball was about 62% using the vibration-assisted polishing process compared with the nonvibrated polishing process.

Keywords: ultrasonic-vibration-assisted ball polishing; ball burnishing; five-axis CNC machining center; Taguchi's experimental method; surface roughness; volumetric wear



Citation: Shiou, F.-J.; Ding, Z.-L.; Lin, S.-P. Reduction in the Volumetric Wear of a Ball Polishing Tool Using Ultrasonic-Vibration-Assisted Polishing Process. *Lubricants* **2022**, *10*, 339. <https://doi.org/10.3390/lubricants10120339>

Received: 3 November 2022

Accepted: 26 November 2022

Published: 30 November 2022

Publisher's Note: MDPI stays neutral with regard to jurisdictional claims in published maps and institutional affiliations.



Copyright: © 2022 by the authors. Licensee MDPI, Basel, Switzerland. This article is an open access article distributed under the terms and conditions of the Creative Commons Attribution (CC BY) license (<https://creativecommons.org/licenses/by/4.0/>).

1. Introduction

Surface finishing processes, such as fine milling, grinding, burnishing, polishing, lapping, and diamond turning, play an important role in the final fabrication stage to improve the surface finish of molds, optical components, and some semiconductor components. The different kinds of polishing machine tools or processes, mainly including the ultraprecision freeform polishing machine, ultrasonic-vibration-assisted polishing, hydrodynamic polishing, abrasive fluid jet polishing, robot-assisted polishing, laser polishing, and sequential ball burnishing and ball polishing, etc., have been discussed in [1]. The main application areas of ultraprecision plane or freeform surface polishing are the fabrication of high-precision optics, artificial orthopedic joints, wafers of semiconductor applications, and precision molds for different kinds of materials. Ultrasonic-vibration assisted polishing processes have been applied to different materials, such as the BK7 or K9 optical glasses, aluminum ceramic, 4H-SiC wafers, sapphire, monocrystalline silicon, Inconel 718 nickel-based alloy, and STAVAX mold steel, etc., to improve the surface roughness of the workpieces. The modeling and analysis of the material removal rate and predictive and experimental research on the polishing slurry consumption model of ultrasonic-vibration-assisted polishing of optical glass BK7 have been presented in [2,3]. The modeling and prediction of the generated local surface profile for ultrasonic-vibration-assisted polishing of optical glass BK7 has been reported in [4]. The predictive modeling and experimental study of the polishing force of ultrasonic-vibration-assisted polishing of K9 optical glass has been reported in [5]. The material removal profile prediction and experimental validation for obliquely axial ultrasonic-vibration-assisted polishing of K9 optical glass

has been investigated in [6]. The effect of ultrasonic-vibration-assisted polishing on the surface properties of alumina ceramic has been investigated in [7]. For the surface finish of 4H-SiC wafers, an efficient and slurryless ultrasonic-vibration-assisted electrochemical mechanical polishing has been proposed in [8]. The effects of ultrasonic amplitude on sapphire ultrasonic-vibration-assisted chemical mechanical polishing has been investigated by experimental and CFD methods [9]. The effect of ultrasonic vibration polishing on the surface quality and material removal rate of monocrystalline silicon has been analyzed in [10]. The ultrasonic-vibration-assisted polishing of Inconel 718 has been studied in [11,12], in which the material removal rate was improved and the surface roughness and average standard deviation of the roughness values significantly reduced. Ultrasonic-vibration-assisted magnetic compound fluid polishing has been developed for the final finishing of acrylic plate in [13]. Using an ultrasonic-vibration-assisted polishing machine, the ultraprecision finishing of a microspheric surface was possible [14,15]. Four different types of CBN particles used to polish STAVAX mold steel on a three-axis machining center, using ultrasonic-vibration-assisted polishing, yielded a better surface finish [16].

The ball burnishing process has been applied to perform the prefinishing process for ball polishing to improve the surface roughness of the mold steel [17]. Using the sequential ball burnishing and ball polishing process, the surface roughness of a workpiece can be improved sequentially from about $1.0\ \mu\text{m}$ to $0.020\ \mu\text{m}$ on average [18]. To reduce the volumetric wear of the polishing ball, a vibration-assisted polishing device for the workpiece, activated by a piezoelectric actuator, was designed and fabricated in [19]; however, the developed device was not suitable for integration with an automated production due to taking up too much space.

With the development of an ultrasonic tool with holder type BT40 that can be integrated into the tool magazine, the automated ultrasonic-vibration-assisted polishing on a machining center is possible, as shown in Figure 1. According to the literature survey, the optimal ultrasonic-vibration-assisted ball polishing parameters for STAVAX mold steel on a five-axis machining center, such as the vibration amplitude, working frequency, spindle speed, abrasive grain size, slurry concentration, depth of penetration, etc., have not been studied.

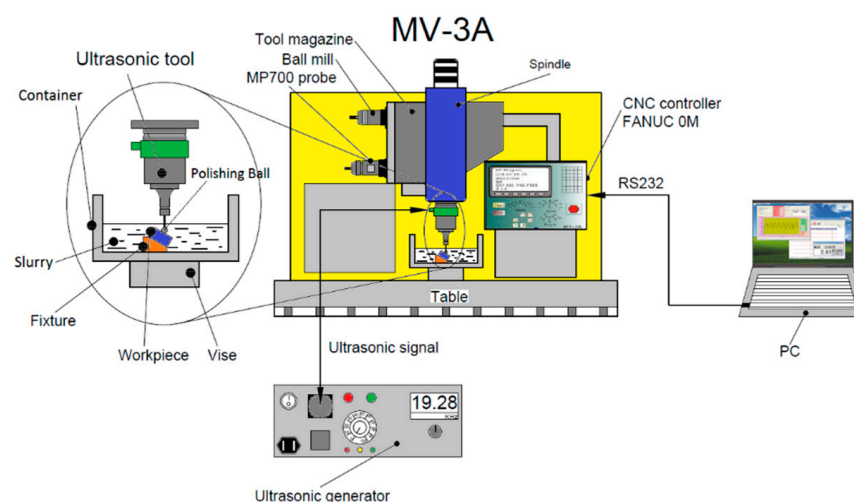


Figure 1. Schematic illustration of the ultrasonic-vibration-assisted ball polishing on a CNC machining center.

The aim of this study was mainly to determine the optimal combination of the ultrasonic-vibration-assisted ball polishing parameters on a machining center and to investigate the tool wear of the polishing ball. The property of the adopted material, STAVAX stainless mold steel, the experimental setup of the ultrasonic-vibration-assisted ball polishing system on a five-axis machining center, and Taguchi's method for determining the optimal plane spherical polishing parameters are introduced in Section 2. The optimal

combination of the ultrasonic-vibration-assisted ball polishing parameters for a plane surface, the ANOVA analysis and discussion on the dominant ultrasonic-vibration-assisted ball polishing factors for plane surfaces, the volumetric wear of the polishing ball, and the application to the surface finishing of an aspherical lens carrier are reported in Section 3. The main results of this study are summarized in conclusion.

2. Materials and Methods

2.1. Materials

The STAVAX stainless mold steel (equivalent to ANSI 420 modified) used in this study combines corrosion and wear resistance with excellent properties in polishing, machinability, and stability in hardening [20]. It can be applied to all type of molds and is especially suited for larger tools where corrosion in production is unacceptable and where high surface finish is required. Table 1 shows the chemical composition of the STAVAX stainless mold steel we used. The hardness of this material is about HRC51 after hardening and tempering.

Table 1. Chemical composition of STAVAX stainless steel (%) [20].

Composition	C	Si	Mn	Cr	V
%	0.38	0.9	0.5	13.6	0.3

2.2. Experimental Setup on a 5-Axis Machining Center

The setup of the experiment for determining the optimal ultrasonic-vibration-assisted ball polishing process parameters is illustrated in Figure 2. The 5-axis machining center we used was fabricated by QUASER Co., (Taichung, Taiwan) type UX300, equipped with the CNC controller of HEIDENHAIN Company (Traunreut, Germany), type iTNC 530. To determine the origin coordinates of the specimen to be machined and perform the intermittent process measurement, a TS740 touch-trigger probe produced by HEIDENHAIN Company was integrated with the machining center tool magazine. The Unigraphics NX10 CAM software (NX10) was used to generate the NC codes required for fine milling, ball burnishing, and spherical polishing path after the simulation. These generated CNC codes were transmitted to the iTNC 530 controller of the machining center through RS232 serial interface. A slurry container with a simple circulation system stirred by an electrical motor was specially designed and mounted on the rotary table. An ultrasonic tool with a maximum vibration amplitude of 15 microns and a working frequency ranging from 18 to 27 kHz was integrated with the machine tool. The Hommelwerke T8000 roughness and contour tester, made by JENOPTIC (Jena, Germany), was used to measure the surface roughness of the fine-milled, burnished, and polished specimens.

The sequential fine milling, ball burnishing, and ultrasonic-vibration-assisted ball polishing processes were adopted in this study for the surface finishing of the specimens and test carrier. The STAVAX (Sweden) specimens were specially designed and manufactured such that they could be mounted on a Kistler (Winterthur, Switzerland) dynamometer to measure the cutting force. The surface to be burnished or polished was divided into eight zones so that the average burnished or polished surface roughness value could be calculated from that of the eight zones. The burnished surface roughness of the fine-milled specimens was 0.122 μm using the optimal ball burnishing parameters. The specimen to be polished was mounted on a fixture with an inclination angle of 45 degrees, as shown in Figure 3, to avoid the stagnation point of the polishing ball clamped on the ultrasonic tool.

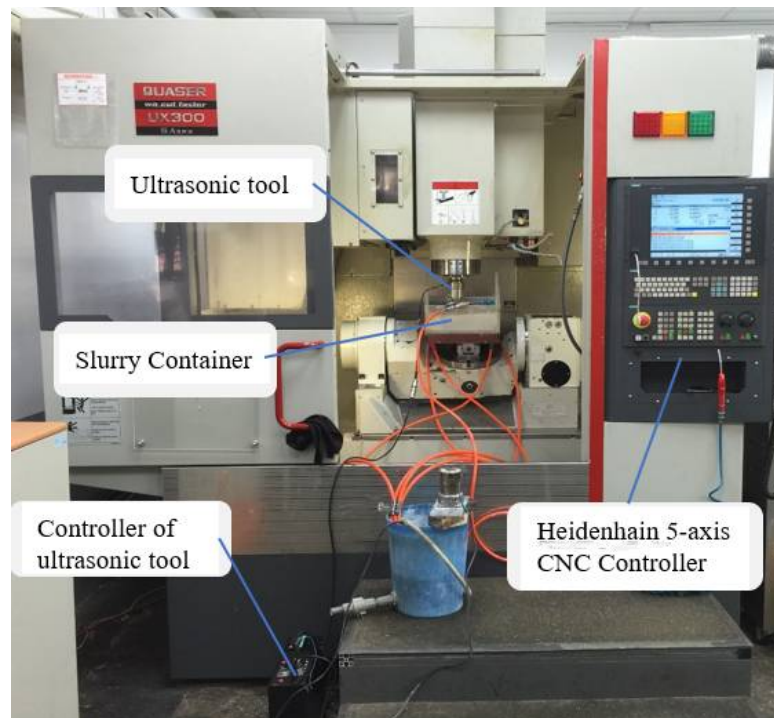


Figure 2. Experimental setup of the ultrasonic-vibration-assisted ball polishing system on the 5-axis machining center.

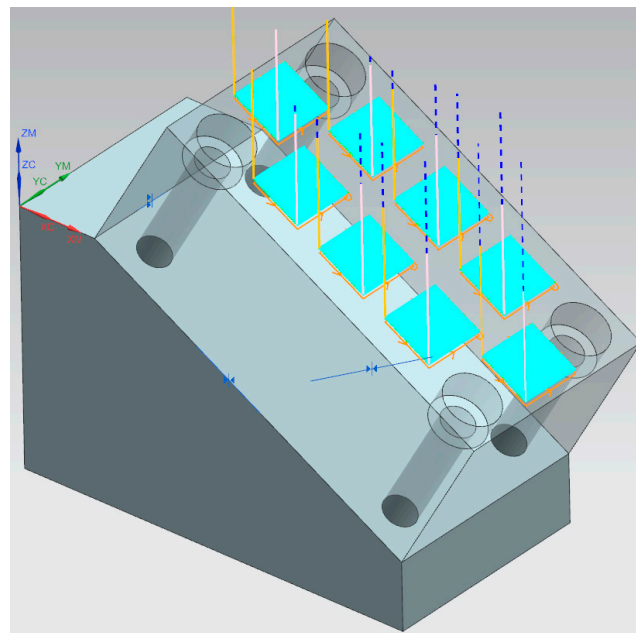


Figure 3. Ultrasonic-vibration-assisted ball polishing path configuration for the specimens.

The amplitude of the ultrasonic tool was measured using an LK-H025 laser displacement meter, a product of KEYENCE Corporation (Osaka, Japan), as shown in Figure 4. The amplitudes of the ultrasonic tool driven by the controller under different working frequencies ranging from 18 kHz to 23 kHz and power ranging from 60 W to 300 W were measured. Figure 5 shows the measured amplitudes of the ultrasonic tool with the power ranging from 60 W to 300 W with the fixed working frequency of 23 kHz. The amplitude was quasi-linearly increased by increasing the power.

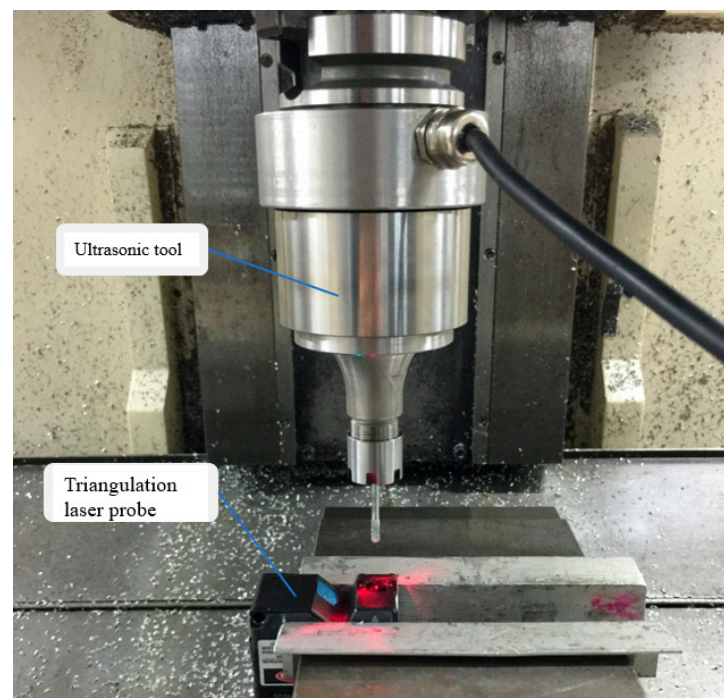


Figure 4. Experimental setup to measure the vibration amplitude of the ultrasonic tool.

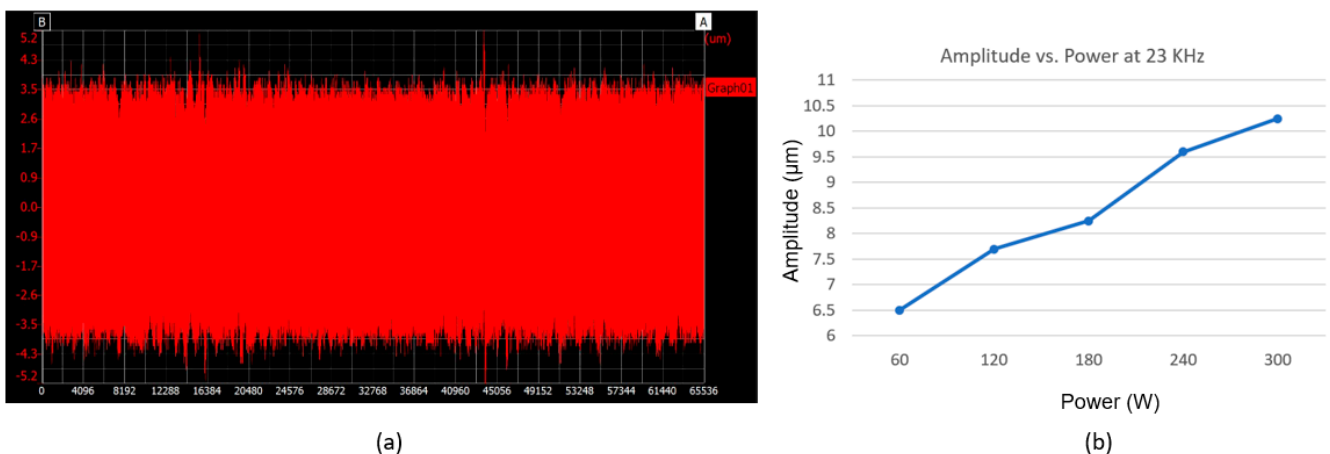


Figure 5. Measured results of the vibration amplitudes of the ultrasonic tool: (a) amplitude of the ultrasonic tool with the working frequency of 23 kHz and power of 300 W; (b) plot of amplitude vs. power.

2.3. Taguchi's Method for Determining the Optimal Plane Spherical Polishing Parameters

2.3.1. Definition of the Data Analysis of Taguchi's Matrix Experiment

To manage the effects of a great number of test parameters, and to ensure the configuration testing is effective, the matrix experiment using Taguchi's orthogonal array is an efficient method to be conducted. As a result, Taguchi's method was adopted to investigate the parameters for the ultrasonic-vibration-assisted ball polishing process to have significant effects on surface roughness. To obtain the optimal spherical polishing parameters, the L18 orthogonal array was used to conduct the matrix experiment in this study.

The quality loss function proposed by Dr. Genichi Taguchi can be classified into the smaller-the-better type, nominal-the-best type, and larger-the-better type [21]. The signal-to-noise (S/N) ratio is used as the objective function to optimize a product or process design. The surface roughness value of the polished surface, using the optimal combination of the polishing parameters, should be less than that of the original surface. Accordingly,

the ultrasonic-vibration-assisted ball polishing process is an example of a smaller-the-better type problem. The S/N ratio, η , is defined by the following equation [21]:

$$\eta = -10\log_{10}(\text{mean square quality characteristic}) = -10\log_{10}\left[\frac{1}{n}\sum_{i=1}^n y_i^2\right] \quad (1)$$

y_i : observations of the quality characteristic under different noise conditions.

n : number of experiments.

The optimization strategy of the smaller-the-better problem is to maximize η defined by Equation (1). Levels that maximize η will be selected for the factors that have a significant effect on η . The optimal conditions for ball polishing can then be determined.

The value of η under the optimal conditions, denoted by η_{opt} , can be predicted by the following equation:

$$\eta_{opt} = m + \sum(m_i - m) \quad (2)$$

η_{opt} : S/N ratio under the optimum conditions.

m : overall mean value of η for the experimental region.

m_i : η under optimal condition for i th factor.

The repeatability and improvement are ideal if the predicted η is very close (in general, 90%) to the experimental η under the optimal conditions and there is no interaction between the factors.

2.3.2. Configuration of the Factors and Levels of Taguchi's Matrix Experiment

The control factors and levels of the vibration-assisted ball polishing process have been configured with an L18 ($2^1 \times 3^7$) orthogonal table with one factor for two levels and seven factors for three levels [21] to obtain the optimal parameters for the ball polishing of STAVAX stainless steel. The configuration table is shown in Table 2. In total, eight main factors, namely, the amplitude, frequency, and spindle speed for the ultrasonic tool, abrasive diameter, feed rate, stepover, depth of concentration, and abrasive concentration, were selected and studied. The abrasive material used in this research was aluminum oxide (Al_2O_3) with the diameters of 0.05 μm , 0.3 μm , and 1.0 μm . The slurry concentrations, made by mixing the abrasive materials with water, were 1:10, 1:20, and 1:30. Three numerical values of each factor were determined based on the prestudy results and the previous research results [17–19]. The L18 orthogonal array was selected to conduct the matrix experiments for seven 3-level factors and one 2-level factor of the ultrasonic-vibration-assisted ball polishing process. The plan of the experiments using the L18 ($2^1 \times 3^7$) orthogonal table is presented in Table 3.

Table 2. Factors and levels of the Taguchi experiments.

Factor	Level 1	Level 2	Level 3
A. Amplitude (μm)	6	10	-
B. Frequency (KHz)	18	20	23
C. Spindle Speed (rpm)	1000	3000	5000
D. Abrasive Diameter (μm)	0.05	0.3	1
E. Feed Rate (mm/min)	20	40	60
F. Stepover (μm)	20	40	60
G. Depth of Penetration (μm)	60	120	180
H. Abrasive Concentration	1:10	1:20	1:30

Table 3. Plan of the experiments using L18 (21×37) orthogonal table.

Expt. No.	Experiment Factor							
	A	B	C	D	E	F	G	H
1	A1	B1	C1	D1	E1	F1	G1	H1
2	A1	B1	C2	D	E2	F2	G2	H2
3	A1	B1	C3	D	E3	F3	G3	H3
4	A1	B2	C1	D	E2	F2	G3	H3
5	A1	B2	C2	D	E3	F3	G1	H1
6	A1	B2	C3	D	E1	F1	G2	H2
7	A1	B3	C1	D	E1	F3	G2	H3
8	A1	B3	C2	D	E2	F1	G3	H1
9	A1	B3	C3	D	E3	F2	G1	H2
10	A2	B1	C1	D	E3	F2	G2	H1
11	A2	B1	C2	D	E1	F3	G3	H2
12	A2	B1	C3	D	E2	F1	G1	H3
13	A2	B2	C1	D	E3	F1	G3	H2
14	A2	B2	C2	D	E1	F2	G1	H3
15	A2	B2	C3	D	E2	F3	G2	H1
16	A2	B3	C1	D	E2	F3	G1	H2
17	A2	B3	C2	D	E3	F1	G2	H3
18	A2	B3	C3	D	E1	F2	G3	H1

3. Experimental Results

3.1. Results of the Optimal Combination of the Ultrasonic-Vibration-Assisted Ball Polishing Parameters for a Plane Surface

Using Equation (1), the S/N ratio of each L18 orthogonal array was calculated with respect to the surface roughness mean value Ra of three tests, as listed in Table 4, after the 18 matrix experiments were executed. The mean surface roughness value Ra ranged from 0.020 μm to 0.067 μm . This can be considered an approximate estimation of the improvement in surface roughness at the best and worst modes. The plot of the average S/N ratio for each level of the eight factors is shown in Figure 6. In general, they are the separate effects of each factor and called main effects. The calculated mean S/N ratio was 27.302 dB, and the mean surface roughness was 0.044 μm , according to the data in Figure 6.

Table 4. Polished surface roughness and calculated S/N ratio.

Exp	Measured Ra Value (μm)			S/N Ratio η (dB)	Mean (μm)
	1	2	3		
1	0.07	0.06	0.06	23.946	0.063
2	0.04	0.03	0.04	28.643	0.037
3	0.06	0.05	0.05	25.426	0.053
4	0.06	0.07	0.07	23.500	0.067
5	0.03	0.04	0.03	29.456	0.033
6	0.04	0.05	0.05	26.576	0.047
7	0.06	0.05	0.05	25.426	0.053
8	0.04	0.05	0.05	26.576	0.047
9	0.04	0.03	0.04	28.643	0.037
10	0.04	0.05	0.05	26.576	0.047
11	0.04	0.04	0.05	27.212	0.043
12	0.03	0.04	0.03	29.456	0.033
13	0.05	0.05	0.05	26.576	0.047
14	0.06	0.06	0.05	24.904	0.057
15	0.03	0.04	0.04	28.643	0.037
16	0.05	0.04	0.05	26.576	0.047
17	0.04	0.04	0.05	27.212	0.043
18	0.02	0.02	0.02	33.979	0.020

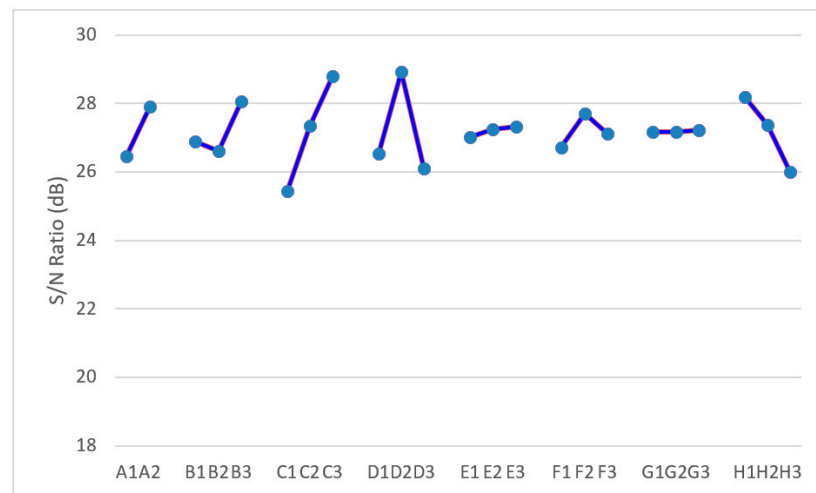


Figure 6. Plots of control factor effects.

The objective in the ultrasonic-vibration-assisted ball polishing process is to minimize the surface roughness value of the polished specimens by determining the optimal level of each factor. Given that $-\log$ is a monotone decreasing function, to maximize it the S/N ratio is required. As a result, we can determine the optimal level for each factor as being the level that has the maximum value of η . The combination of the optimal level for each factor was A2B3C3D2E3F2G3H1, based on Figure 6.

The optimal combination of the ultrasonic-vibration-assisted ball polishing parameters is summarized in Table 5. The amplitude of the ultrasonic tool was 10 μm ; the working frequency of the ultrasonic tool was 23 kHz; the spindle speed was 5000 rpm; the diameter of the aluminum oxide (Al_2O_3) was 0.3 μm ; the feed rate was 60 mm/min; the stepover distance was 20 μm ; depth of penetration was 180 μm ; and the slurry concentration was 1:10.

Table 5. Combination of the optimal ultrasonic-vibration-assisted ball polishing parameters.

Factor	Level
A. Amplitude (μm)	10
B. Frequency (KHz)	23
C. Spindle Speed (rpm)	5000
D. Abrasive Diameter (μm)	0.3
E. Feed Rate (mm/min)	60
F. Stepover (μm)	20
G. Depth of Penetration (μm)	180
H. Abrasive Concentration	1:10

Three verification experiments were carried out to determine the repeatability of using the optimal combination of the spherical polishing parameters. The surface roughness of $R_a = 22$ nanometers (nm) on average, measured by the Hommelwerke (VS-Schwenningen, Germany) T8000 surface roughness measuring equipment, as shown in Figure 7, can be obtained based on the confirmation test results. The surface roughness improvement in the tested object from the burnished surface to the polished surface was about $(0.122 - 0.022)/0.122 = 81.96\%$. Using the same polishing parameters without the ultrasonic vibration, the surface roughness of $R_a = 28$ nanometers on average can be obtained according to the test results. It could then be confirmed that the combination of the level for each factor was the set of optimal parameters for the ultrasonic-vibration-assisted ball polishing of STAVAX stainless mold steel.

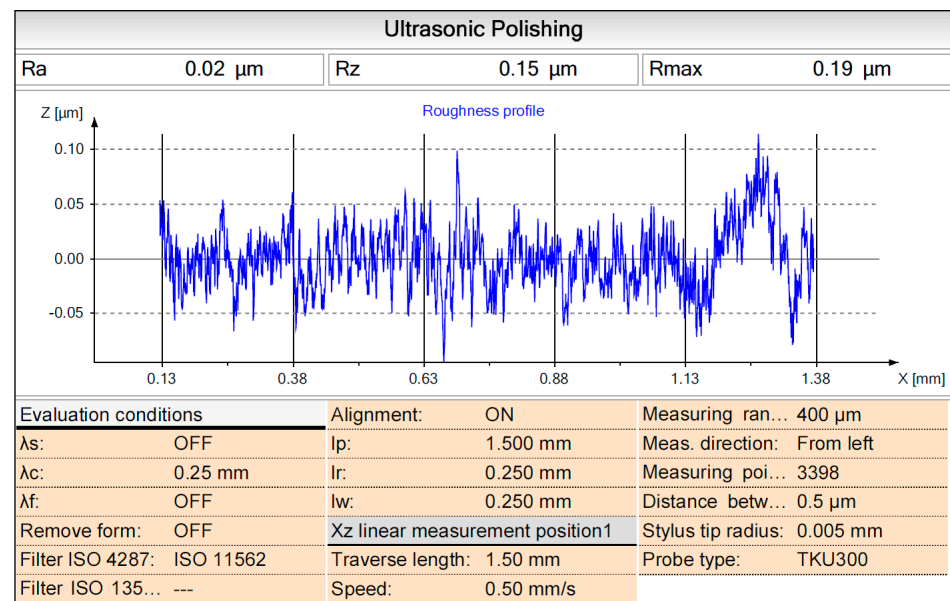


Figure 7. Measured surface roughness of the specimen using the determined ball polishing parameters.

The calculated S/N ratio of the mean surface roughness was 32.638 dB. The predicted S/N ratio η_{opt} under optimal conditions was 33.735 dB, calculated by using Equation (2) according to the data in Figure 6, which is very close (about 96.75%) to the experimental S/N ratio $\eta = 32.638$ dB under the optimal ball polishing conditions. Accordingly, there is no interaction among the selected factors.

3.2. ANOVA Analysis and Discussion on the Dominant Ultrasonic-Vibration-Assisted Ball Polishing Factors for Plane Surface

The main effect of each factor was further determined by using the analysis of variance (ANOVA) technique and the F ratio test in order to find out the significant factors (Table 6). The ratio value of $F_{0.05, 2, 9}$ is 4.26 for a level of significance equal to 0.05 (or 95% confidence level); the factor's degree of freedom is 2 and the degree of freedom for the pooled error is 9 according to the F-distribution table [22]. The F ratio values that are greater than 4.26 can be concluded as having a significant effect on surface roughness. As a result, the amplitude, working frequency, and spindle speed of the ultrasonic tool, the abrasive diameter, and the slurry concentration played the most significant roles on surface roughness improvement among the ultrasonic-vibration-assisted ball polishing parameters.

Table 6. ANOVA analysis for S/N ratio of the polished surface roughness using the ultrasonic-vibration-assisted ball polishing parameters.

Factor	D.F.*	S.S.*	M.S.*	F*	T.S.*	Contribution
A. Amplitude	1	6.522	6.522	12.543	6.002	6.529%
B. Frequency	2	6.441	3.221	6.194	5.401	5.876%
C. Spindle Speed	2	34.407	17.204	33.088	33.367	36.298%
D. Abrasive Diameter	2	24.102	12.051	23.177	23.062	25.087%
E. Feed Rate	2	0.340	-	-	-	-
F. Stepover	2	2.040	-	-	-	-
G. Depth of Penetration	2	0.154	-	-	-	-
H. Abrasive Concentration	2	14.256	7.128	13.709	13.216	14.377%
Error	2	3.615	-	-	-	-
Total (SST)	17	91.927	-	-	-	-
Pooled to Error	9	4.159	0.520	-	-	-

D.F.*: degree of freedom; S.S.*: sum of squares; M.S.*: mean of squares; F*: variance ratio; T.S.*: total sum of squares.

Discussion on the significant factors: With an increase in the vibration amplitude, more abrasive particles could be sucked into the instantaneous gap between the polishing ball and the specimen surface, resulting in the effective polishing of the surface. However, the higher amplitude might have had a greater contact surface, causing the wear of the polishing ball. Similarly, more abrasive particles could be drawn into the instantaneous gap between the polishing ball and the specimen surface when the vibration frequency increased, improving the surface roughness. Nevertheless, the working frequency ranging from 18 kHz to 23 kHz had no obvious effect on the surface roughness improvement, as shown in Figure 6. The spindle speed had the greatest contribution (36%) on the surface roughness improvement, for the greater velocity field could be generated near the polishing ball when the rotational speed of the ultrasonic tool increased, resulting in a better polishing effect. The rotational speed of the ultrasonic tool we used was restricted up to 6000 rpm. The diameter of 0.3 μm of the abrasive was more optimal than the diameter of 1.0 μm for the improvement of the surface roughness. Nonetheless, the burnished mark could not be removed using the diameter of 0.05 μm of the fine abrasive. A possible reason is that the fine abrasive grains were embedded into the cavities between the peaks and the valleys of the burnished surface with a roughness of R_a 0.122 μm , such that the effective polishing of the surface could not be obtained. The lower the slurry concentration, the better the abrasive worked on material removal to improve the surface roughness.

3.3. Volumetric Wear of the Polishing Ball

To evaluate the volumetric wear of the polishing tool, a solid model of the used polishing tools was constructed using a coordinate measuring machine to measure the profile of the polishing ball with wear and the SolidWorks CAD software (SolidWorks 2016) for solid model construction. The constructed solid model is shown in Figure 8a,b. It shows that the volumetric wear of the polishing ball can be reduced by about 62.5% with ultrasonic-vibration-assisted polishing. The reason for the reduction in the volumetric wear was that the total sliding path had been reduced due to the intermittent contact between the vibrating polishing ball and the surface of the workpiece.

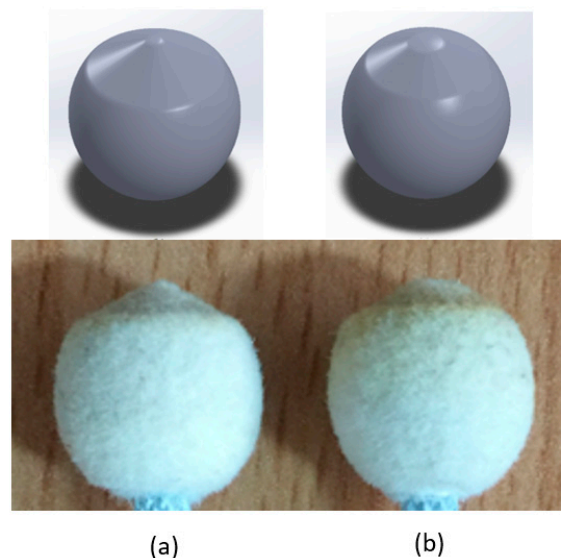


Figure 8. Comparison of the volumetric wear of the used polishing balls and their CAD model (a) with no ultrasonic vibration and (b) with ultrasonic vibration.

3.4. Application to the Surface Finishing of an Aspherical Lens Carrier

The determined optimal ball burnishing and spherical polishing parameters for plane surfaces were sequentially applied to the surface finishing of an aspherical lens carrier (Figure 9a) constructed by a reverse engineering process. The surface roughness R_a of the freeform surface region on the STAVAX tested part, which was hardened and tempered

(HRC = 51), can be improved sequentially from about 0.272 μm to 0.014 μm (Figure 9b). The 3D surface roughness of the test carrier was measured with a Taylor Hobson (Leicester, England) white light interferometer, type Talysurf CCI 6000. The surface roughness value Ra on the fine-milled surface of the test object was 0.272 μm on average. The surface roughness value Ra on the burnished surface was 0.107 μm on average. The surface roughness value Ra on the ultrasonic-vibration-assisted polished surface was 0.014 μm ($R_t = 0.097 \mu\text{m}$), as shown in Figure 10, whereas the surface roughness Ra on the no-vibration-assisted polished surface was 0.017 μm on average. The surface roughness improvement of the tested object on the burnished surface was about 61%, and that on the ultrasonic-vibration-assisted polished surface was about 87%. The volumetric wear of the polishing ball can be reduced by about 59.3% with ultrasonic-vibration-assisted polishing.

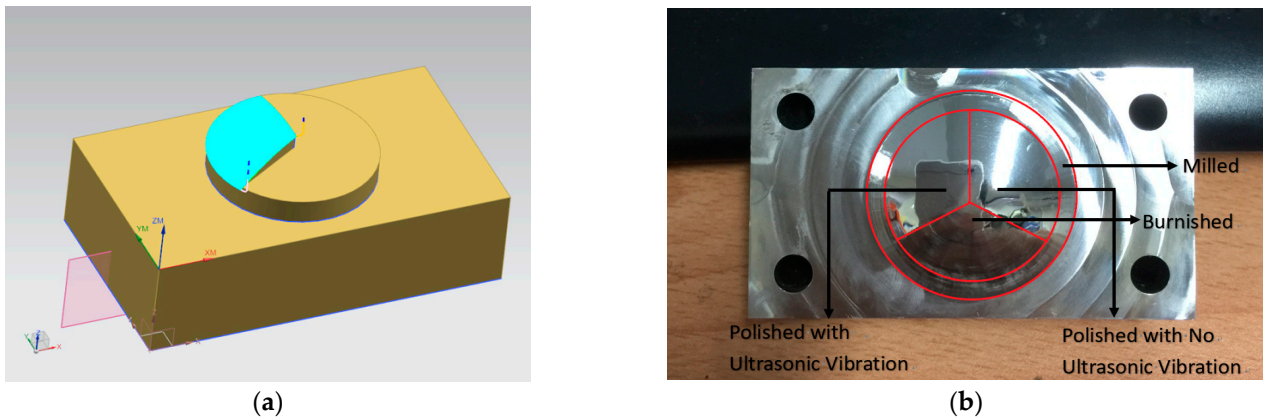


Figure 9. (a) Machining path simulation for the constructed CAD model of the aspherical lens carrier (b) Comparison of the polished aspherical lens carrier using the ultrasonic-vibration-assisted ball polishing and with no vibration.

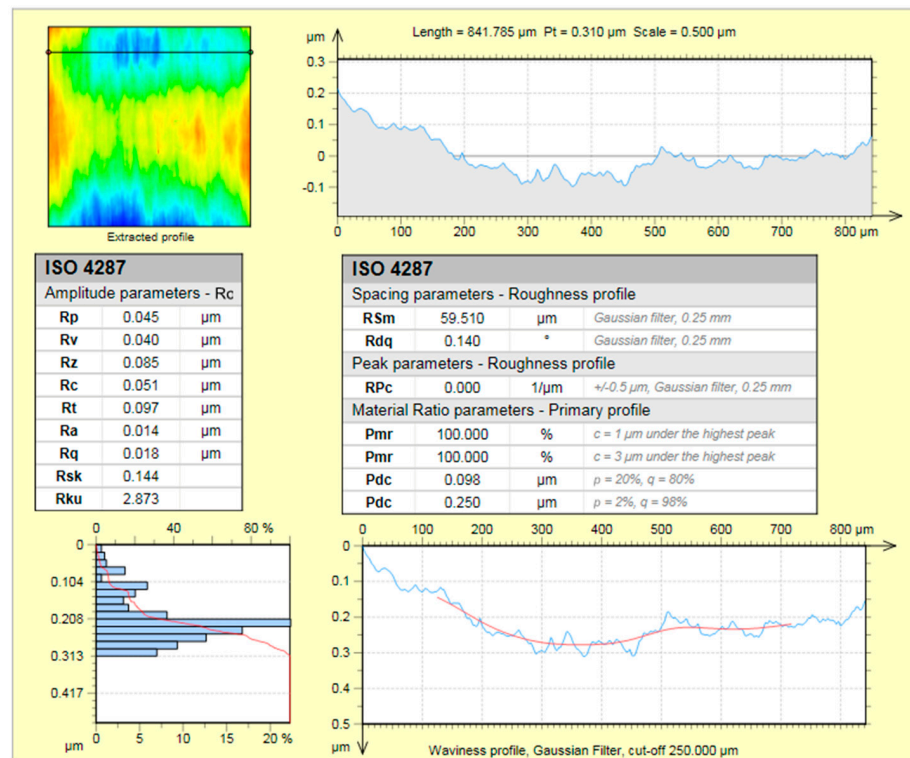


Figure 10. Measured surface roughness of the polished aspherical lens carrier using the ultrasonic-vibration-assisted ball polishing.

4. Conclusions

An ultrasonic-vibration-assisted ball polishing process on a five-axis machining center was successfully developed and the volumetric wear of the polishing ball was investigated in this study. The main results of this study can be summarized as follows:

1. According to the Taguchi L18 matrix experimental results, the optimal combination of the ultrasonic-vibration-assisted ball polishing parameters for the STAVAX mold steel was an amplitude of 10 μm , working frequency of 23 KHz, rotational speed of 5000 rpm, abrasive particle size of 0.3 μm , feed rate of 60 mm/min, stepover of 20 μm , depth of penetration of 180 μm , and ratio of polishing liquid of 1:10.
2. The surface roughness Ra of the burnished plane specimen was improved from about 0.122 μm to 0.022 μm using the optimal combination of the ultrasonic-vibration-assisted ball polishing parameters.
3. The volumetric wear of the polishing ball for a plane surface was reduced by about 62.5% with ultrasonic-vibration-assisted polishing, based on the constructed CAD models of the used polishing balls.
4. The proposed optimal plane ball polishing parameters were applied to the surface finishing of an aspherical lens carrier. The surface roughness improvement of the tested object on the ultrasonic-vibration-assisted polished surface was about 87%. The volumetric wear of the polishing ball was reduced by about 59.3% with ultrasonic-vibration-assisted polishing.

Author Contributions: F.-J.S. contributed to the conceptualization, methodology, project administration, and paper writing; Z.-L.D. contributed to the implementation of the experiment, data collection and analysis, and draft writing in Chinese; S.-P.L. contributed to the supervision of the operation of the machine tool and CNC code verification. All authors have read and agreed to the published version of the manuscript.

Funding: This research has been sponsored by the Ministry of Science and Technology of the Republic of China (Taiwan) under grant MOST 108-2221-E-011-153-MY3.

Acknowledgments: The authors are grateful to Taiwan Tech for providing the research facilities.

Conflicts of Interest: The authors declare no conflict of interest.

References

1. Shiou, F.J.; Tsegaw, A.A. Ultra precision surface finishing processes. *Int. J. Autom. Technol.* **2019**, *13*, 174–184. [[CrossRef](#)]
2. Liang, Y.; Zhang, C.; Chen, X.; Zhang, T.; Yu, T.; Zhao, J. Modeling and analysis of the material removal rate for ultrasonic vibration-assisted polishing of optical glass BK7. *J. Adv. Manuf. Technol.* **2022**, *118*, 627–639. [[CrossRef](#)]
3. Liang, Y.; Chen, X.; Niu, J.; Zhang, C.; Ma, Z.; Xu, P.; Li, M.; Yu, T.; Zhao, J. Predictive and experimental research on the polishing slurry consumption model for ultrasonic vibration-assisted polishing of optical glass BK7. *Ceram. Int.* **2022**, *48*, 10048–10058. [[CrossRef](#)]
4. Zhang, T.; Wang, Z.; Yu, T.; Chen, H.; Dong, J.; Zhao, J.; Wang, W. Modeling and prediction of generated local surface profile for ultrasonic vibration-assisted polishing of optical glass BK7. *Ceram. Int.* **2021**, *47*, 19809–19823. [[CrossRef](#)]
5. Zhang, C.; Qu, S.; Liang, Y.; Chen, X.; Zhao, J.; Yu, T. Predictive modeling and experimental study of polishing force for ultrasonic vibration-assisted polishing of K9 optical glass. *J. Adv. Manuf. Technol.* **2022**, *119*, 3119–3139. [[CrossRef](#)]
6. Qu, S.; Wang, Z.; Zhang, C.; Ma, Z.; Zhang, T.; Chen, H.; Wang, Z.; Yu, T.; Zhao, J. Material removal profile prediction and experimental validation for obliquely axial ultrasonic vibration-assisted polishing of K9 optical glass. *Ceram. Int.* **2021**, *47*, 33106–33119. [[CrossRef](#)]
7. Zhang, C.; Liang, Y.; Cui, Z.; Meng, F.; Zhao, J.; Yu, T. Study on the effect of ultrasonic vibration-assisted polishing on the surface properties of alumina ceramic. *Ceram. Int.* **2022**, *48*, 21430–21447. [[CrossRef](#)]
8. Yang, X.; Yang, X.; Gu, H.; Kawai, K.; Arima, K.; Yamamura, K. Efficient and slurryless ultrasonic vibration assisted electrochemical mechanical polishing for 4H-SiC wafers. *Ceram. Int.* **2022**, *48*, 7570–7583. [[CrossRef](#)]
9. Zhou, M.; Zhong, M.; Xu, W. Effects of ultrasonic amplitude on sapphire ultrasonic vibration assisted chemical mechanical polishing by experimental and CFD method. *Mech. Adv. Mater. Struct.* **2021**, *in press*. [[CrossRef](#)]
10. Yu, T.; Wang, Z.; Guo, X.; Xu, P.; Zhao, J.; Chen, L. Effect of ultrasonic vibration on polishing monocrystalline silicon: Surface quality and material removal rate. *J. Adv. Manuf. Technol.* **2019**, *103*, 2109–2119. [[CrossRef](#)]
11. Yu, T.; Guo, X.; Wang, Z.; Xu, P.; Zhao, J. Effects of the ultrasonic vibration field on polishing process of nickel-based alloy Inconel 718. *J. Mater. Process. Technol.* **2019**, *273*, 116228. [[CrossRef](#)]

12. Yu, T.; Yang, X.; An, J.; Yu, X.; Zhao, J. Material removal mechanism of two-dimensional ultrasonic vibration assisted polishing Inconel 718 nickel-based alloy. *J. Adv. Manuf. Technol.* **2018**, *96*, 657–667. [[CrossRef](#)]
13. Nomura, M.; Ozasa, K.; Fujii, T.; Suzuki, T.; Wu, Y. Development of Ultrasonic Vibration-Assisted Magnetic Compound Fluid (MCF) Polishing Technology. *J. Adv. Manuf. Technol.* **2022**, *16*, 71–77. [[CrossRef](#)]
14. Suzuki, H.; Moriwaki, T.; Okino, T.; Ando, Y. Development of Ultrasonic Vibration Assisted Polishing Machine for Micro Aspheric Die and Mold. *CIRP Ann.-Manuf. Technol.* **2006**, *55*, 385–388. [[CrossRef](#)]
15. Suzuki, H.; Hamada, S.; Okino, T.; Kondo, M.; Yamagata, Y.; Higuchi, T. Ultraprecision Finishing of Micro-aspheric Surface by Ultrasonic Two-axis Vibration Assisted Polishing. *CIRP Ann.-Manuf. Technol.* **2010**, *59*, 347–350. [[CrossRef](#)]
16. Tsai, M.Y.; Lin, Y.F.; Ho, J.K.; Yang, J.G. Ultrasonic vibration-assisted innovative polyurethane tool to polish mold steel. *Int. J. Autom. Technol.* **2019**, *13*, 199–206. [[CrossRef](#)]
17. Shiou, F.; Cheng, C. Ultra-precision Surface Finish of NAK80 Mold Tool Steel Using Sequential Ball Burnishing and Ball Polishing Processes. *J. Mater. Process. Technol.* **2008**, *201*, 554–559. [[CrossRef](#)]
18. Shiou, F.; Hsu, C. Surface Finishing of Hardened and Tempered Stainless Tool Steel Using Sequential Ball Grinding, Ball Burnishing and Ball Polishing Processes on a Machining Center. *J. Mater. Process. Technol.* **2008**, *205*, 249–258. [[CrossRef](#)]
19. Shiou, F.J.; Ciou, H.S. Ultra-precision surface finish of the hardened stainless mold steel using vibration-assisted ball polishing process. *Int. J. Mach. Tools Manuf.* **2008**, *48*, 721–732. [[CrossRef](#)]
20. STAVAX ESR. Available online: https://www.assab.com/app/uploads/sites/133/2020/04/Stavax_ESR_PH-EN.pdf (accessed on 25 October 2022).
21. Phadke, M.S. *Quality Engineering Using Robust Design*; Pearson: Karnataka, India, 2015.
22. Montgomery, D.C. *Design and Analysis of Experiments*; Wiley: New York, NY, USA, 2019.